Inhibitory effects of Moringa oleifera leaves extract on xanthine oxidase activity from bovine milk

by Hasnah Natsir

Submission date: 20-Apr-2022 09:09PM (UTC+0700)
Submission ID: 1815435623
File name: PHAR_article_77740_en_1_Published.pdf (2.04M)
Word count: 9154
Character count: 48961

PHARMACIA

Pharmacia 69(2): 363–375
DOI 10.3897/pharmacia.69.e77740

Research Article

Inhibitory effects of *Moringa oleifera* leaves extract on xanthine oxidase activity from bovine milk

Hasnah Natsir[1], Abdur Rahman Arif[1], Abdul Wahid Wahab[1], Prastawa Budi[1], Rugaiyah Andi Arfah[1], Arwansyah Arwansyah[2], Ahmad Fudholi[3,4], Ni Luh Suriani[5], Achmad Himawan[6]

1 *Department of Chemistry, Faculty of Mathematics and Natural Sciences, Hasanuddin University, Makassar 90245, Indonesia*
2 *Department of Chemistry Education, Faculty of Teacher Training and Education, Tadulako University, Palu, Indonesia*
3 *Universiti Kebangsaan Malaysia, 43600 Bangi, Selangor, Malaysia*
4 *National Research and Innovation Agency Republic of Indonesia (BRIN), Bandung, Indonesia*
5 *Biology Study Program, Mathematics and Natural Sciences Faculty, Udayana University, Bali 80361, Indonesia*
6 *Department of Pharmaceutical Science and Technology, Faculty of Pharmacy, Hasanuddin University, Makassar 90245, Indonesia*

Corresponding author: Hasnah Natsir (hasnahnatsir@unhas.ac.id)

Received 8 November 2021 ♦ **Accepted** 10 March 2022 ♦ **Published** 14 April 2022

Citation: Natsir H, Arif AR, Wahab AW, Budi P, Arfah RA, Arwansyah A, Fudholi A, Suriani NL, Himawan A (2022) Inhibitory effects of *Moringa oleifera* leaves extract on xanthine oxidase activity from bovine milk. Pharmacia 69(2): 363–375. https://doi.org/10.3897/pharmacia.69.e77740

Abstract

Moringa oleifera is a tropical plant in the Moringaceae family that contains a lot of bioactive compounds. This study aimed to isolate and characterize the enzyme xanthine oxidase (XO), and conducted inhibitory tests on XO using methanol extracts of *M. oleifera* leaves. The xanthine oxidase enzyme isolated from bovine milk was characterized to determine the optimum pH, temperature, and substrate concentration. XO inhibition was evaluated by *in vitro* and *in silico* methods. The results of XO isolation and characterization of bovine milk showed the optimum conditions at pH 6.5, substrate concentration of 0.1 mM, and temperature 35 °C with an activity rate of 32.47 mU/mL; 21.55 mU/mL, and 21.94 mU/mL. Inhibition analysis results on methanol extract of *M. oleifera* leaves showed the highest activity decrease at the extract concentration of 160 ppm, with a relative inhibition value of 21.35%, while allopurinol as a positive control has a relative value inhibition of 61.21%. Relative value inhibition indicated the potential of *M. oleifera* leaves as a source of medicinal plants for gout sufferers. Additionally, a computational analysis was performed to observe the molecular interaction between the primary compounds of *M. oleifera* leaves, i.e., 5-O-acetyl-thio-octyl-β-L-rhamnofuranoside, quinic acid, and 2-diethyl(trimethylsilylmethyl)silyloxymethyltetrahydrofuran, and XO using the molecular docking method. The finding implied that these compounds are bound to the catalytic sites of XO by hydrogen bonds and hydrophobic interactions, indicating the primary compounds of *M. oleifera* leaves could become XO inhibitors to treat gout disease.

Keywords

Moringa oleifera leaves, inhibition, molecular docking, xanthine oxidase, bovine milk

Introduction

Moringa oleifera is a medicinal plant that is widely cultivated in many tropical and subtropical countries (Boopathi and Raveendran 2021). *M. oleifera* is a beneficial plant because its certain parts, such as leaves, flowers, roots, seeds, and fruits, are widely used in a variety of applications. *M. oleifera* leaves, flowers and fruits are used as vegetables and traditional medicines. *M. oleifera* seed is a natural coagulant that can be used to purify water and as an oil extraction agent in the production of biofuel (Sagona et al. 2020). While, according to several studies *M. oleifera* root has antibacterial, antioxidant, and antidiabetic properties (Tshabalala et al. 2020). Currently, *M. oleifera* study focused on the leaf medical benefits. The diversity of metabolites in the leaves is indicated to have several pharmacological actions. A number of studies show that the flavonoid and phenolic compounds found in *M. oleifera* leaves have antidiabetic, antibacterial, antimicrobial and anti-inflammatory activities. Several studies suggest that the flavonoid and phenolic compounds in *M. oleifera* leaves have anti-inflammatory, antidiabetic, antibacterial, and antifungal activities (Fejér et al. 2019); antiulcer activity is provided by sterols, terpenoids, flavonoids, tannins, and glycosides in *M. oleifera* leaves (Jincy and Sunil 2020), whereas antioxidant activity is provided by polyphenols (Padayachee and Baijnath 2020; Rocchetti et al. 2020). Furthermore, *M. oleifera* leaves other pharmacological properties include its capacity to block enzymes that act as receptors for particular diseases (Singh et al. 2020).

XO is an enzyme that plays a role in catalyzing the oxidation of hypoxanthine to xanthine, which becomes uric acid. XO is derived from the enzyme class molybdenum iron-sulfur flavin hydroxylase, mainly found in the liver, kidneys, brain, gastrointestinal tract (Maiuolo et al. 2016). The enzyme is also present in the entire cardiovascular system. Inhibition of XO can suppress the biosynthesis of uric acid, which is one of the therapeutic approaches for treating gout, neuropathy, and kidney stones, which leads to hyperuricemia (Gliozzi et al. 2016; White 2018).

Suppressing XO activity is the primary approach in treating hyperuricemia and gout in clinical settings because XO has an essential role in the formation of uric acid. Allopurinol, a synthetic drug used clinically to treat gout, is one of the XO inhibitors. (Seth et al. 2014). However, excessive use of allopurinol can cause nephropathy, hepatitis, digestive disorders, reduced white blood cells, allergies, and liver damage (Zeng et al. 2018). In order to avoid these undesirable side effects, the use of medicinal plants can be considered as an alternative therapeutic option (Mohos et al. 2019).

One of the plants that indicated to have the ability in inhibiting XO activity is *M. oleifera*. Based on our previous study, *M. oleifera* leaves contain secondary metabolites such as flavonoids, alkaloids, tannins, and saponins. Methanolic extract of *M. oleifera* leaves showed antioxidant activity and inhibition of the α-glucosidase enzyme (Natsir et al. 2018, 2019). This study aimed to analyze the inhibitory activity of methanol extract of *M. oleifera* leaves against XO enzyme isolated from bovine milk. However, the XO enzyme was isolated and characterized first in order to determine the optimal conditions of the enzyme. Moreover, the molecular docking method was employed to investigate insight into the molecular recognition of the primary compounds of *M. oleifera* leaves in binding to the moiety of XO (Blaney and Dixon 1993; Kitchen et al. 2004).

Materials and methods

Chemicals and instruments

The materials used in this study included: bovine milk obtained from cattle farmers in Enrekang Regency, South Sulawesi, *M. oleifera* leaf from Topoyo Subdistrict, West Sulawesi Province (2°02'17.21"S, 114°15'30.36"E), $CH_3OH_{(pa)}$, NaCl, $(NH_4)_2SO_4$, $NaOH_{(pa)}$, HCl, xanthine substrate and allopurinol were purchase from Sigma Aldrich. The instruments used in this study were autoclave, centrifuge (Hermle Z336K), Alu-Lid rotor (Hermle 220.87 V20), rotary evaporator, vortex, stirrer magnetic, UV-Vis 1800 (Shimadzu-Japan), FTIR Spectrophotometer (Shimadzu-Japan), GCMS-QP2010 Ultra (Shimadzu-Japan).

Isolation of XO

The XO isolation process is a modified method from Bou-Salah (Bou-Salah et al. 2020), in which 500 mL fresh bovine milk was heated to a temperature of 30 °C, combined with 178.5 g of NaCl, then centrifuged at a speed of 3000 rpm for 30 minutes. The supernatant was fractionated with ammonium sulfate at 4 °C using an ice bath, then centrifuged at 8000 rpm at 4 °C for 20 minutes using a Alu-Lid rotor (RFC 21.379/24.325 xg; angle rotor 24 × 1.5/2.0 mL; angle 45°, maximum speed 15.000/16.000 rpm). The precipitate was dissolved in 0.05 M potassium phosphate buffer pH 7.5 to 250 mL.

Preparation of XO Solution

Xanthine substrate of about 15.21 mg was added to the measuring flask and then added with five drops of 1 M NaOH, shaken until dissolved. The solution was diluted with CO_2-free demineralized water to 100.0 mL (1 mM concentration). The xanthine substrate was prepared by diluting the stock solution to obtain a standard solution, with a concentration of 0.05; 0.1; 0.15; 0.2, and 0.25 mM (Kostić et al. 2015).

Allopurinol solution

Allopurinol 1000 µg/mL stock solution was prepared by weighing 10 mg of allopurinol and dissolving it in 5 drops of 1 M NaOH. The solution was transferred to a volumetric flask with a volume of 10 mL and then diluted with CO_2-free demineralized water. The standard allopurinol

solution was prepared by diluting the stock solution to get a series of allopurinol standard solutions, with a concentration of 0.1; 0.2; 0.5; 1.0 and 2.0 µg/mL (Gong et al. 2020).

XO crude extract

The crude XO extract was weighed about 22.17 mg using a 25 mL weighing bottle, then the extract was added into a volumetric flask and diluted with phosphate buffer solution. The volume was diluted to the limit mark to obtain an XO solution of 0.1 U/mL (Kostić et al. 2015).

XO characterization

The crude extract of the enzyme was characterized to determine the optimum conditions of the enzyme, such as pH, substrate concentration, and temperature effect (Natsir et al. 2002; Kostić et al. 2015). The optimum conditions were determined by analyzing the optimum activity of the enzyme. It was calculated by equation 1:

$$Ea = \frac{(Ab - Ac)V \times df}{12.2 \times 0,1} \quad (1)$$

Where Ea is enzyme activity (mU/mL); Ab is the absorbance of blank; Ac is the absorbance of control; V is total volume assay (mL); df is dilution factor; 12.2 is uric acid extinction coefficient at 290 nm (mM); and 0.1 is the volume of XO used in milliliter (mL).

Optimum pH

Phosphate buffer solutions of 0.2 M (3.9 mL) with a pH variation of 6; 6.5; 7; 7.5 and 8 were added 2 mL of 0.15 mM xanthine substrate solution, then pre-incubated for 10 minutes at 25 °C. 0.1 mL of XO was added to the mixtures and then incubated for 30 minutes at 25 °C. The absorption of the sample was measured at λ_{max} 232 nm using a UV-Vis spectrophotometer (Natsir et al. 2002; Kostić et al. 2015; Sharma et al. 2016).

Optimum substrate concentration

The optimum substrate concentration was determined by adding 2 mL of phosphate buffer solution at the optimum pH, with a xanthine substrate concentration of 0.05; 0.10; 0.15; 0.20, and 0.25 mM. After pre-incubation, 0.1 mL of XO was added to the solution, and the mixture was incubated at 25 °C for 30 minutes. A similar procedure was applied for control by replacing the crude enzyme extract using 0.1 mL of distilled water (Natsir et al. 2002; Kostić et al. 2015).

Optimum temperature

Phosphate buffer solution 0.2 M (3.9 mL) of optimum pH was added to 2 mL of xanthine substrate with optimum concentrations, and then pre-incubated for 10 minutes. The enzyme XO (0.1 mL) was added, incubated for 30 minutes at 20; 25; 30; 35, and 40 °C. After the incubation process, the absorption was measured at λ_{max} of 232 nm using a UV-Vis spectrophotometer (Natsir et al. 2010; Monika et al. 2019).

Preparation and extraction *Moringa oleifera* leaves

M. oleifera leaves were harvested from the tree by manually collecting the 3rd to 5th petiole leaves. The leaves were washed and then dried for 7–10 days at room temperature. After drying, the leaves were then processed into a fine powder using a grinding machine. Dry *M. oleifera* leaves powder was mixed with methanol in a ratio of 1:20 (w/v). The extraction process was conducted at 45 °C for 20 minutes with constant stirring using a magnetic stirrer. The extract obtained was filtered and then evaporated using a rotary evaporator to obtain a thick methanol extract. The metabolomic profile of the methanol extract was analyzed using FTIR and GCMS (Natsir et al. 2018, 2019; Rocchetti et al. 2019).

FTIR spectroscopic analysis

The FTIR spectrum of *M. oleifera* leaves methanol extract was analyzed using an FTIR spectrophotometer (Shimadzu-Japan) at a wavenumber of 4000–250 cm^{-1}. The spectrum was recorded using approximately 1 mg of methanol extract (Meenakshi et al. 2020).

GCMS analysis

The methanol extract of *M. oleifera* leaves was analyzed using GCMS-QP2010 Ultra (Shimadzu), which was connected to a capillary column DB-1 (0.25 m film 0.25 mm I. d. 30 m length). The temperature of the injector was kept at 250 °C (constant). The column oven temperature was set at 50 °C for 3 minutes, then raised to 280 °C for 3 minutes, and finally held at 300 °C for 10 minutes. The chromatogram results were identified by comparing the obtained spectral configurations on mass spectral databases that were readily available (NIST libraries) (Ezhilan and Neelamegam. 2012).

Inhibition activity of methanol extract of *Moringa oleifera* leaves against XO

The methanol extract of *M. oleifera* leaves were diluted to a 10, 20, 40, 80 and 160 µg/mL concentrations with 0.05 mM phosphate buffer solution pH 7.5. An aliquot of 3 mL extract solution was added to a reaction tube, followed by 2 mL of 0.15 mM xanthine and 0.2 mL of XO, and then incubated at room temperature for 45 minutes. After incubation, 1 mL HCl (0.58 M) was added to the mixtures to stop the enzymatic reaction. Water was used as the control solution for the negative control, and allopurinol as a positive control. The absorbance of the solution was measured using a UV-Vis spectrophotometer at λ_{max} of

232 nm. Calculation of inhibition ability was obtained from the linear equation of the time versus concentration of the XO curve (Fachriyah et al. 2018).

Molecular docking

Molecular docking was performed using the AutoDock Vina package developed by Trott and co-workers to determine the ligand's binding site into the receptor's catalytic site (Trott and Olson 2010). In this study, the *M. oleifera* leaves extracts were indicated to treat gout disease induced by hyperuricemia. A study reported that 5-O-acetyl-thio-octyl-β-L-rhamnofuranoside, quinic acid, and 2-dimethyl(trimethylsilylmethyl)silyloxymethyltetrahydrofuran were identified as the primary compounds of *M. oleifera* and therefore used as the ligand molecules for the docking. The chemical structures of those ligands were retrieved from the PubChem database, as shown in Fig. 1. All ligands were downloaded and saved as sdf extensions. Open Babel 2.4.1 program packages were applied to convert sdf files to pdbqt extension (O'Boyle et al. 2011). As for the target molecule, XO was assigned as the receptor since this enzyme is related to gout disease. The receptor's tertiary structure was obtained from a protein data bank (PDB ID: 1v97) at a resolution of 1.94 Å, as shown in Fig. 2 (Okamoto et al. 2004). The polar hydrogen and Kollman's united atom charges were added to the receptor using AutoDock Tools 1.5.6 created by Morris and co-workers (Morris et al. 2009). Afterwards, the XO was saved in pdbqt format.

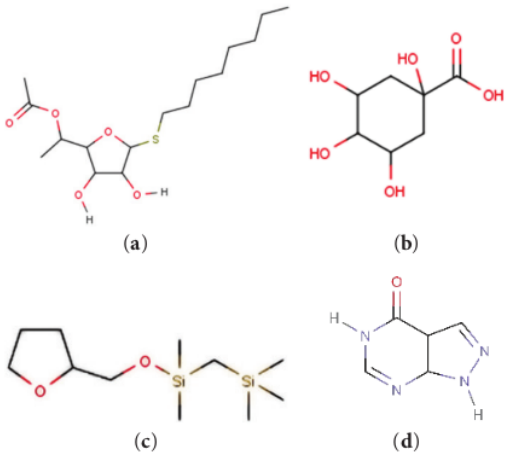

Figure 1. The compounds' chemical structure of (**a**) 5-O-acetyl-thio-octyl-β-L-rhamnofuranoside (PubChem ID: 537841), (**b**) Quinic acid (PubChem ID: 6508), (**c**) 2-Dimethyl(trimethylsilylmethyl)silyloxymethyltetrahydrofuran (PubChem ID: 559105), and (**d**) Allopurinol (PubChem ID: 135401907) as the positive control.

In performing molecular docking, a grid box parameter is required to decide the positional and rotational of the ligand into the moiety of the receptor (Arwansyah et al. 2021a). The grid box was constructed using 24 × 24 26 points and a grid spacing of 1.00 Å. Meanwhile, the grid box's central coordinates were set to x = 148.649, y = 43.411, and z = 26.399. The exhaustiveness was computed at 100. Other parameters were assigned as the default of AutoDock Vina. To determine the binding pose and conformation of the ligand within the receptor site, the Broyden-Fletcher-Goldfarb-Shanno (BFGS) algorithm was used as a search parameter. The docking protocols were set according to a similar procedure with our previous study provided in Ref. (Arwansyah et al. 2021b).

Figure 2. The tertiary structure of the created model of XO (PDB: 1v97) (Okamoto et al. 2004). The structures of α-helix, β-sheet, and turn are presented by cartoon models' red, yellow, and green colours.

Result and discussion

Isolation results from bovine milk produced 340 mL of crude extract of XO enzyme. The enzymes used for the characterization and inhibition tests were stored at 4 °C to maintain stability and avoid denaturation.

Characterization of XO

Determination of the optimum pH of the enzyme was carried out by conditioning the enzyme at a certain pH in the reaction between the enzyme and the substrate, as shown in Fig. 3a. Each type of enzyme has an optimum pH range, where the enzyme offers maximum activity in high stability. Generally, enzymes are amphiphilic, which means they can be acidic and base due to their active ability to provide functional groups of specific amino acid residues that are donor and acceptor proton (Singh et al. 2017). The XO activity showed that the optimum pH was at 6.5 with the activity of 32.47 mU/mL, and after pH increased at pH 7.0, XO activity decreased to 18.10 mU/mL. It was unveiled that the increase of enzyme activity at the optimum pH can be related to changes in ionization of the enzyme ionic group on the active site. Thus the conformation of the active site

becomes more effective in binding and changing the substrate during the catalysis process (Huang et al. 2017).

The effect of substrate concentration was assessed to determine the optimum substrate concentration suitable for the enzyme. The substrate concentration used was 0.05; 0.1; 0.15; 0.2; 0.25 mM. The results obtained are shown in Fig. 3b. The results demonstrated that higher enzyme activity was achieved at elevated substrate concentration. However, when thereafter it reached the optimum substrate concentration, the activity tended to decrease. We reported that the highest enzyme activity was at 0.1 mM substrate concentration, with an activity of 21.55 U/mL. The increase in substrate concentration is directly related to the reaction rate until it reaches a maximum value of V_{max}. If the substrate concentration is increased, there will be no increase in the reaction rate because the substrate has saturated the enzyme's active site (Sharma et al. 2016).

Temperature is critical in enzymatic reactions because enzymes are proteins that are easily denatured against changing environmental conditions. The change in environmental temperature will affect enzyme activity (Claaßen et al. 2019). The enzyme will show optimal catalytic activity at a specific temperature and denatured when exposed to extreme temperatures (Roche and Royer 2018). When the temperature increases to optimal, the reaction rate would be accelerated because kinetic energy increases (Marañón et al. 2018). Increased kinetic energy will accelerate the motion of vibration, translation, and rotation of both enzymes and substrates. It will increase the frequency of collisions between enzymes and substrates (Zhang et al. 2016). In this study, the determination of the optimum temperature of the XO enzyme used a variation of incubation temperature in the range of 20; 25; 30; 35 and 40 °C. The results obtained are shown in Fig. 3c. From the graph, it is clearly seen that the optimum temperature was reached at 35 °C with an activity of 21.94 mU/mL.

FTIR spectroscopic analysis

FT-IR spectroscopic analysis of *M. oleifera* leaves methanol extract was used to analyze the phytoconstituents in the sample based on spectral data (Fig. 4).

The results of the FTIR analysis of the methanol extract of *M. oleifera* leaves (Table 1) showed the presence of flavonoids and phenolics from the O-H and C=O groups at 3435 cm^{-1} and 1732, 1714 cm^{-1} which indicated the presence of C-H stretching. Alkaloids in the C-N band at 1460, 1411 cm^{-1} and N-H in the fingerprint region of 1635 cm^{-1} (Maobe et al. 2013).

Tannins were discovered in the form of free phenol by stretching O-H at 3435 cm^{-1} and C-O at 1238 cm^{-1}. The C=O band is represented by the peak found at 1732, 1714 cm, and the C-O band is represented by the peak found at 1238 cm^{-1}.

GCMS profiling data showed three main compounds in the methanol extract of *M. oleifera* leaves, namely

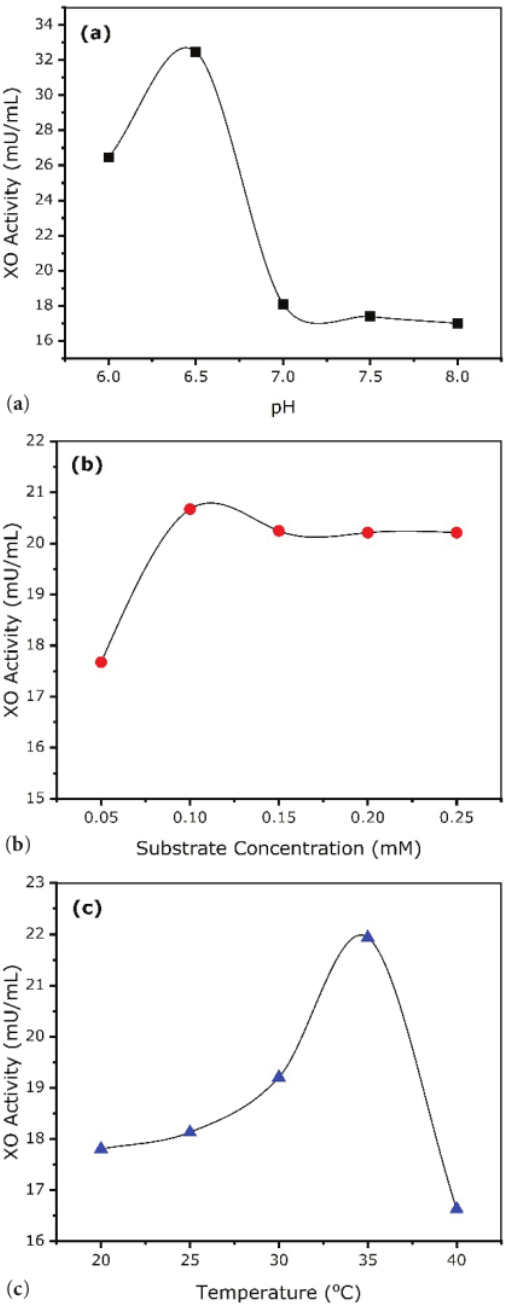

Figure 3. Characterization of XO (**a**) pH; (**b**) Substrate concentration; (**c**) Temperature.

5-O-acetyl-thio-octyl-β-L-rhamnofuranoside, quinic acid, and 2-dimethyl(trimethylsilylmethyl)silyloxymethyltetrahydrofuran. The presence of 5-O-acetyl-thio-octyl-β-L-rhamnofuranoside was identified from the O-H group at 3435 cm^{-1}, C-H at 2924, 2854 cm^{-1}, C=O at 1732,

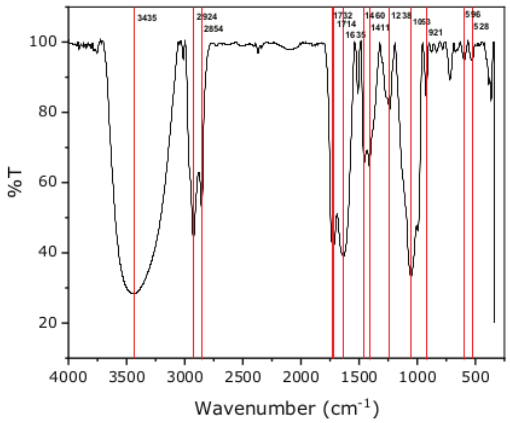

Figure 4. FTIR spectrum of methanol extract of *M. oleifera* leaves.

1714 cm^{-1} and C-O at 1238 cm^{-1} which are stretch in cyclic ethers. The presence of the C-S group at 596 cm^{-1} is a specific band of the 5-O-acetyl-thio-octyl-β-L-rhamnofuranoside compound. Quinic acid was identified from the typical strain O-H at 3435 cm^{-1}, C-O at 1238 cm^{-1}, C-C=O at 528 cm^{-1} and C-OH at 921 cm^{-1} which is a typical band of carboxylic acid groups. The compound 2-dimethyl(trimethylsilylmethyl)silyloxymethyltetrahydrofuran was identified from the presence of C-H band at 2924, 2854 cm^{-1}, C-O at 1238 cm^{-1}, and Si-O-C at 1053 cm^{-1} which are typical bands of this compound.

GCMS analysis

For metabolite profiling, GCMS was used to identify bioactive compounds in a methanol extract of *M. oleifera* leaves. The GCMS chromatogram (Fig. 5) showed 78 peaks which indicating the presence of 78 metabolite compounds.

Tabel 1. FTIR spectra analysis of methanol extract of *M. oleifera* leaves.

Functional groups	Wavenumber (cm^{-1})	Vibrations
O-H	3435	stretch
C-H	2924, 2854	stretch
C=O	1732, 1714	stretch
N-H	1635	bend
C-N	1460, 1411	stretch
C-O	1238	stretch
Si-O-C	1053	stretch
C-OH	921	deformation
C-S	596	stretch
C-C=O	528	bend

The seventy eight compounds are characterized and identified through comparison of constituent mass spectra with the NIST library (Table 2).

The diversity of phytochemical compounds in plant extracts is closely linked to their bioactivity. However, the main compound in the highest concentration appears to play a key role in the medicinal activity of the plant (Huie 2002). Based on the metabolite profile data in Table 2, the main compounds in the methanol extract of *M. oleifera* leaves are 5-O-acetyl-thio-octyl-β-L-rhamnofuranoside (16.53%), quinic acid (14.66) and 2-dimethyl(trimethylsilylmethyl)silyloxymethyltetrahydrofuran (12.21%). This is based on the highest concentration value of each compound, which is more than 10%. The mass spectra of the three main compounds identified in the methanol extract of *M. oleifera* leaves are presented in Fig. 6.

In general, two compounds were reported to have antioxidant activity among the three main compounds, and no activity was reported for 2-dimethyl(trimethylsilylmethyl)silyloxymethyltetrahydrofuran from the samples (Pero 2009; Verma et al. 2019). Besides being an antioxidant, quinic acid has anti-inflammatory (Nam et al. 2019), anti-hepatitis B virus (Wang et al. 2009), and hepatoprotective activities (Kim et al. 2007). The biological activity

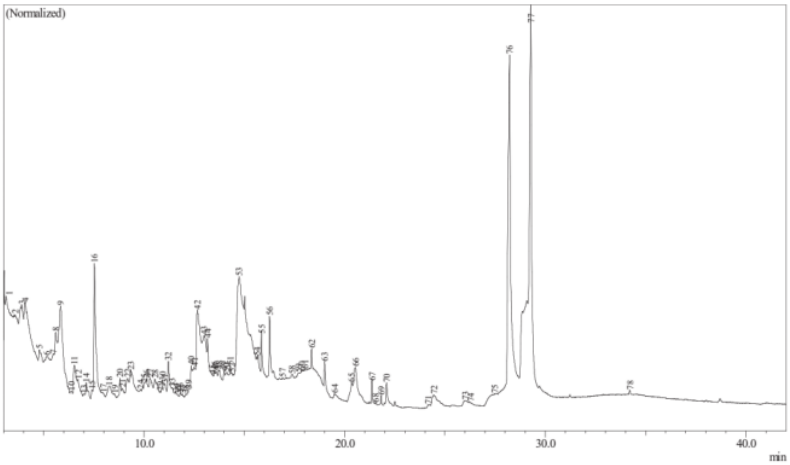

Figure 5. GCMS chromatogram of *M. oleifera* leaves methanol extracts.

Table 2. Phytocomponents identified in the methanol extract of *M. oleifera* leaves by GCMS.

Peak Number	Ret.Time	Name of the compounds	Peak Area (%)
1	3.123	2-Furann[illegible]nol	0.13
2	3.568	2-[3'-(1"-Hydroxy-1"-Methylethyl)-2',2'-Dimethylcyclobutyl] Ethanal	0.06
3	3.903	1,2,4,5-Tetrazine, 1,2,3,6-Tetrahydro-3,6-Dimethyl-	0.71
4	4.079	[illegible]utanamine, 2-Methyl-N-(2-Methylbutylidene)-	1.34
5	4.779	2,4-Dihydroxy-2,5-Dimethyl-3(2H)-furan-3-one	0.25
6	5.161	6-(t-butyloxycarbonylaminopropionamido)hexanamide, N-methyl-N-[4-(1-pyrrolidinyl)-	0.49
7	5.467	N-Methyl-3-piperidinecarboxamide	0.41
8	5.594	1-Butanamine, 2-Methyl-N-(2-Methylbutylidene)-	0.97
9	5.84	[illegible],4-Butanetetrol, [S-(R*,R*)]-	2.9
10	6.374	2-Octenoic acid, 4,5,7-trhydroxy	0.03
11	6.522	1,3,5-Triazine-2,4,6-triamine	0.77
12	6.708	Cyclopentanol	0.32
13	6.992	Benzeneethanol	0.04
14	7.116	[illegible],8,10-Tetraoxaspiro[5.5]undecane	0.29
15	7.4	2-Propanamine, N-Methyl-N-Nitroso-	0.12
16	7.524	4H-Pyran-4-one, 2,3-dihydro-3,5-dihydroxy-6-methyl-	3.31
17	7.975	alpha-[5-Ethyl-2,3,4,5-tetrahydro-2-furyl]glycine	0.03
18	8.262	5-Methoxypyrrolidin-2-one	0.42
19	8.533	Butylamine, N-(1-Propylbutylidene)-	0.05
20	8.804	Boron, Trihydro(Morpholine-N4)-, (T-4)-	0.32
21	8.923	2,3-Dihydro-Benzofuran	0.22
22	9.183	2-Furancarboxaldehyde, 5-(hydroxymethyl)-	0.6
23	9.349	2-Propanone, 1-Phenyl-	1.31
24	9.819	Prednisolone	0.26
25	10	2-Chloroethyl vinyl sulfide	0.39
26	10.118	Cyclohexanone, 2-(2-Butynyl)-	0.51
27	10.312	[illegible]-Pyrrolidione, N-[2-(thienyl)acetyloxy]-	0.67
28	10.545	[illegible]anoic acid, 2-[(tetrahydro-2H-pyran-2-yl)oxy]-	0.76
29	10.808	2-Propanone, 1-(3,5,5-trimethyl-2-cyclohexen-1-ylidene)-, (Z)-	0.09
30	10.922	2-Methyl-l-methylmannopyranoside	0.4
31	11.033	[illegible]peridineacetic Acid, .Alpha.-Phenyl-, Methyl Ester	0.28
32	11.213	2-Furanmethanol, 5-ethenyltetra[illegible]ro-.alpha.,.alpha.,5-trimethyl-, cis-	0.83
33	11.4	Naphthalene, 1,2-Dihydro-1,5,8-Trimethyl-	0.25
34	11.592	Ethanone, 1-(2,3-Dihydro-1,1-Dimethyl-1h-Inden-4-[illegible]-	0.12
35	11.683	4-(2,4,4-Trimethyl-cyclohexa-1,5-dienyl)-but-3-en-2-one	0.05
36	11.809	1,6,6-Trimethyl-7-(3-oxobut-1-enyl)-3,8-dioxatricyclo[5.1.0.0(2,4)]octan-5-one	0.12
37	11.917	[illegible]0-Dimethylene-Tricyclo[4.2.1.1 2,5]Decane	0.08
38	12.075	4-(7,8-Di[illegible]ro-Tetrazolo[1,5-B][1,2,4]Triazin-7-Yl)-2,6-Dimethyl-Phenol	0.12
39	12.225	Bi[illegible][4.2.1]nona-2,4,7-triene, 9-acetyl-, syn-	0.17
40	12.352	4-(2,4,4-Trimethyl-1,5-Cyclohexadien-1-Yl)-3-Buten-2-One	0.55
41	12.505	Undecane, 3-Methyl-	0.97
42	12.653	[illegible]enzeneacetonitrile, 4-hydroxy-	3.61
43	12.994	[illegible]D-Glucopyranose, 1,6-Anhydro-	2.44
44	13.166	2(4H)-Benzofuranone, 5,6,7,7a-tetrahydro-4,4,7a-trimethyl-, (R)-	1.66
45	13.417	[illegible]ecanoic Acid	0.32
46	13.512	1,3-Cyclohexanediol, 2,5-Dimethyl-2-nitro-, monoacetate (ester), [1s-(1.alpha.,2.β.,3.alpha.,5.alpha.)]-	0.42
47	13.594	[illegible]enediamide, N-Dodecyl-N'-(2-Thiazolyl)-	0.53
48	13.759	1,2-Benzenedicarboxylic Acid, Diethyl Ester	1.03
49	13.994	1,3,3-Trimethyl-2-(2-Methylcyclopropyl)-1-Cyclohexene #	0.53
50	14.095	3-Buten-2-one, 1-(2,3,6-trimethylphenyl)-	0.65
51	14.3	[illegible]rgastigmatrienone	0.79
52	14.375	3[illegible]hyl-6-Oxo-2-Hexenyl Acetate	0.3
53	14.742	[illegible],4,5-Tetrahydroxy-Cyclohexanecarboxylic Acid (Quinic Acid)	14.66
54	15.626	10,11-Dihydroxy-3,7,11-Trimethyl-2,6-Dodecadienyl Acetate	1.52
55	15.867	[illegible]adecanoic acid	1.75
56	16.262	2[illegible]-Benzofuranone, 5,6,7,7a-Tetrahydro-6-Hydroxy-4,4,7a-Trimethyl-, (6s-Cis)-	3.1
57	16.906	3,7,11,15-Tetramethyl-2-hexadecen-1-ol	1.17
58	17.367	[illegible]tyl 2-(8-Methylnonyl) Phthalate #	2.13
59	17.7	Ethanone, 1,1'-(5-Hydroxy-2,2-Dimethylbicyclo[4.1.0]Heptane-1,7-Diyl)Bis-, (1.Al	1.03
60	17.867	[illegible]tyl-.β.-D-glucopyranoside	0.92
61	18.017	5-(Diethylamino)-3,4-Dimethyl-2(5h)-Furanone #	1.6

Peak Number	Ret.Time	Name of the compounds	Peak Area (%)
62	18.353	Hexadecanoic Acid, Methyl Ester	3.39
63	19.008	n-Hexadecanoic acid	1.04
64	19.5	Hexadecanoic acid, ethyl ester	0.17
65	20.35	Nonanoic Acid	0.53
66	20.539	ctadecenoic Acid (Z)-	1.47
67	21.364	9-Octadecenoic acid (Z)-, methyl ester	0.22
68	21.55	2-Hexadecen- , 3,7,11,15-Tetramethyl-, [R-[R*,R*-(E)]]-	0.02
69	21.817	Octadecanoic acid, methyl ester	0.09
70	22.091	11,14,17-Eicosatrienoic acid, methyl ester	0.44
71	24.167	Geranyl isovalerate	0.08
72	24.443	Benzyl .β.-d-glucoside	0.73
73	26.017	2-Methyl-3-(2-Methylphenyl)Propanal	0.25
74	26.267	Sclareolide	0.12
75	27.483	2-Methyl-1-[3-(1-Trimethylsilanyloxy-Pentyl)-Oxiranyl]-Propan-1-Ol	0.78
76	28.22	2-Dimethyl(trimethylsilylmethyl)silyloxymethyltetrahydrofuran	12.21
77	29.279	5-O-Acetyl-Thio-Octyl-β-L-Rhamnofuranoside	16.53
78	34.219	Hexatriacontane	0.06

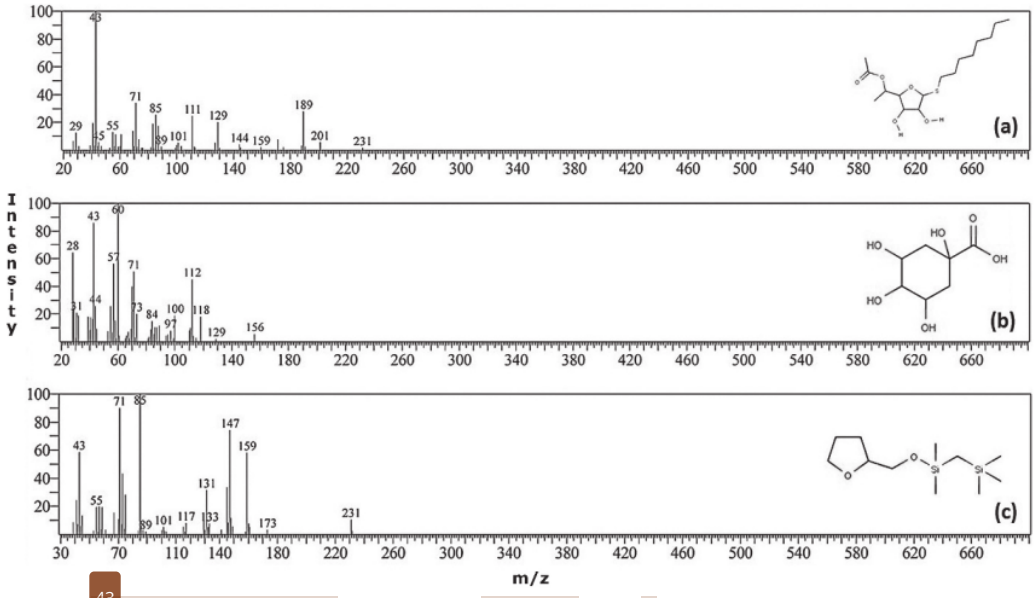

Figure 6. Mass spectrum and structure of main compounds identified by GCMS in the methanol extract of *M. oleifera*: **(a)** 5-O-acetyl-thio-octyl-β-L-rhamnofuranoside; **(b)** Quinic acid; **(c)** 2-Dimethyl(trimethylsilylmethyl)silyloxymethyltetrahydrofuran.

of each compound is a function of its lipophilic properties, functional group properties, and its solubility in methanol (Ezhilan and Neelamegam 2012).

Inhibition of methanol extract of *Moringa oleifera* leaves against XO activity

Various concentrations of enzyme were used in the inhibition assay to determine the relationship between increasing enzyme concentration and inhibition activities. We reported that the methanol extracts of *M. oleifera* leaves demonstrated in vitro XO inhibition activity, and the results are presented in Table 3.

The analysis inhibition showed that the effectiveness of inhibition was directly proportional to the increase in extract concentration. Methanol extract at a concentration of 10 mg/mL showed inhibition values of 5.73%, while at a 160 mg/mL concentration, the inhibition value was 21.35%. The increased inhibitory activity of the methanol extract of *M. oleifera* leaves was significantly linked with the metabolite content of the leaves. The presence of three

Table 3. The inhibition value of methanol extract of *M. oleifera* leaves against XO.

Sample concentrations (mg/mL)	Methanol extract inhibition (%)
10	5.73
20	7.04
40	8.83
80	10.02
160	21.35
Negative control	0
Allopurinol (positive control)	62.11

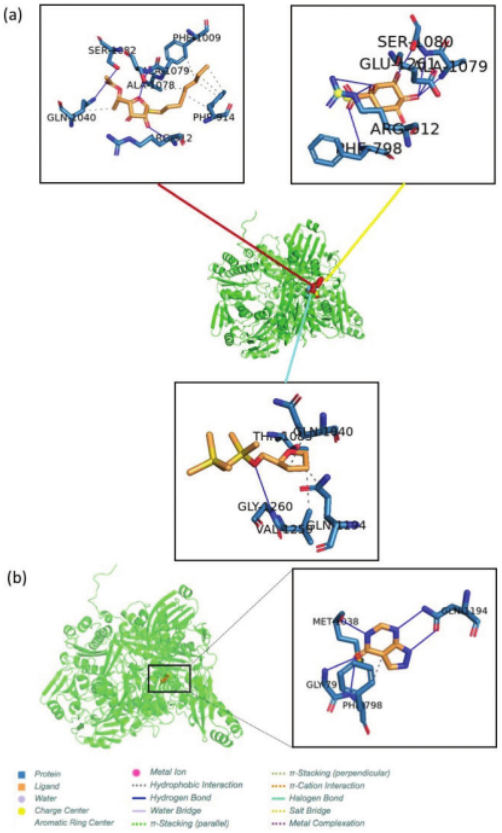

Figure 7. Binding poses of ligand in complex with a receptor (XO). Complex 1 consisted of mixed compounds where the red, yellow, and cyan lines refer to 5-O-acetyl-thio-octyl-β-L-rhamnofuranoside, quinic acid, and 2-dimethyl(trimethylsilylmethyl) silyloxymethyltetrahydrofuran compounds, respectively, (b) complex 2 denoted to allopurinol (control). The PLIP program (Salentin et al. 2015) and Pymol v 2.3 program packages (DeLano. 2002) was used to display the conformational poses of each complex.

Table 4. The binding energy of ligands in a complex with a receptor (XO) is obtained by molecular docking.

No.	Compound	Binding Energy (Kcal/mol)
1	5-O-acetyl-thio-octyl-β-L-rhamnofuranoside	-8.2
2	Quinic acid	-6.7
3	2-Dimethyl(trimethylsilylmethyl) silyloxymethyltetrahydrofuran	-3.6
4	Allopurinol	-6.6

main compounds in the methanol extract of *M. oleifera* leaves namely is 5-O-acetyl-thio-octyl-β-L-rhamnofuranoside, quinic acid, and 2-dimethyl(trimethylsilylmethyl) silyloxymethyltetrahydrofuran, become a constituent that works to prevent substrates from entering the enzyme's active site.

The mechanism for binding the substituent to the active site of the XO enzyme occurs through the interaction of the O-H, C=O and C-H aliphatic functional groups of the three main compounds through hydrogen bonds and hydrophobic interactions. The interaction mechanism can be seen in Fig. 5. Another study investigating the potential of *M. oleifera* leaves constituents as XO inhibitors were conducted by Tian et al (2021) who studied the enzymatic hydrolysis of phenolic and peptide fractions of *M. oleifera* leaves. It was discovered that the hydrolysis process significantly increased the inhibitory activity of XO as well as the antioxidant activity. These findings in the present study showed methanol extract of *M. oleifera* leaves activity indicating a promising potential for its development as an XO inhibitor.

Molecular docking analysis

To analyze the molecular recognition concerning the inhibitory activity, an advanced experimental investigation by X-ray analysis is required to obtain insight into the molecular interaction, including binding energy between the extraction of *M. oleifera* leaves and the tested enzyme (XO). However, computational analysis using the molecular docking method can currently investigate the struc-

Table 5. The hydrogen bonds of ligand in complex with the receptor.

Complex	Residue	AA	Distance H-A (Å)	Distance D-A (Å)	Donor Angle	Donor Atom	Acceptor Atom
Complex 1 (Fig. 8a)	912A	Arg	3.47	3.8	101.02	8316 [Nam]	12332 [O3]
	1040A	Gln	2.05	3.05	164.93	9569 [Nam]	12341 [O2]
	1080A	Ser	2.54	3.28	129.26	9925 [Nam]	12331 [O3]
	1082A	Ser	2.68	3.06	104.92	9947 [O3]	12341 [O2]
Complex 2 (Fig. 8b)	912A	Arg	2.73	3.14	103.89	8324 [Ng+]	12333 [O3]
	912A	Arg	3.7	4.01	100.18	8330 [Ng+]	12333 [O3]
	1079A	Ala	2.37	3.12	129.44	9919 [Nam]	12341 [O3]
	1080A	Ser	3.15	3.96	136.91	9925 [Nam]	12341 [O3]
	1080A	Ser	2.52	2.88	102.01	12343 [O3]	9931 [O3]
	1261A	Glu	3.16	3.61	109.99	12341 [O3]	11647 [O2]
Complex 3 (Fig. 8c)	1083A	Thr	2.23	2.86	123.24	9955 [O3]	12338 [O3]
	1260A	Gly	3.57	3.97	105.81	11634 [Nam]	12335 [O3]
Control (Fig. 8d)	797	Gly	1.87	2.8	150.6	7210 [N]	12327 [O2]
	798	Phe	2.22	3.1	143.5	7215 [N]	12327 [O2]
	1038	Met	2.29	2.88	115.99	12337 [N]	9550 [O2]
	1194	Gln	1.95	2.96	172.11	11022 [N]	12335 [N2]
	1194	Gln	2.04	2.96	149.52	12332 [Npl]	11021 [O2]

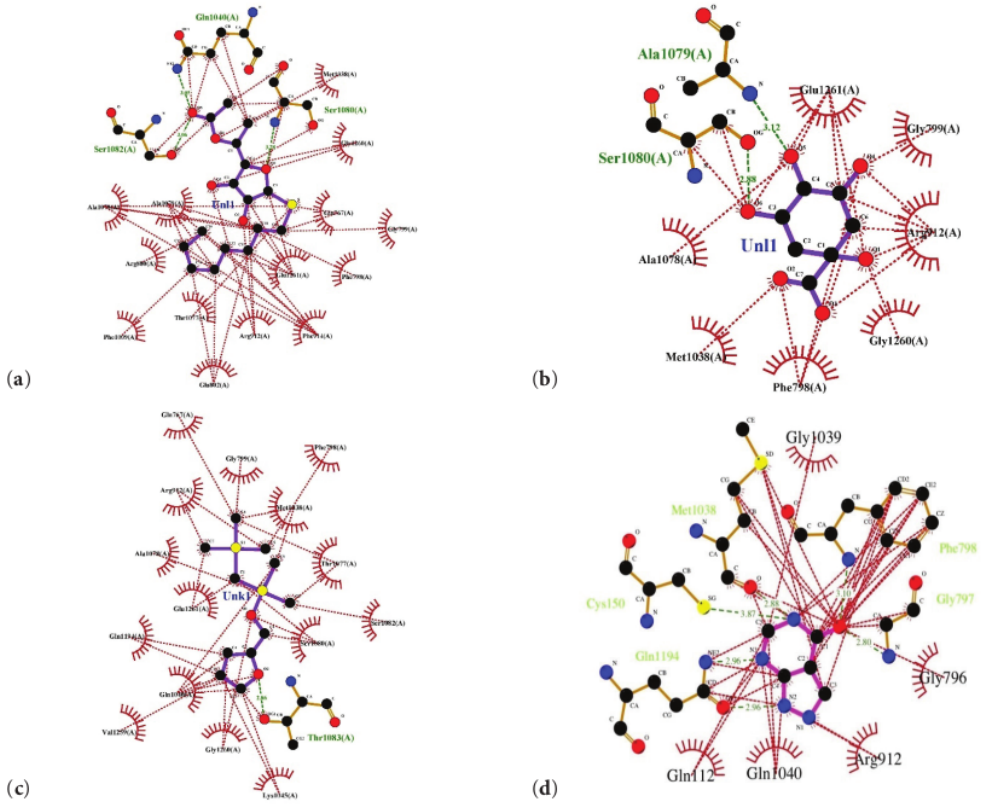

Figure 8. Hydrophobic interaction of ligand in complex with the receptor. (**a**) 5-O-acetyl-thio-octyl-β-L-rhamnofuranoside, (**b**) Quinic acid, (**c**) 2-Dimethyl(trimethylsilylmethyl)silyloxymethyltetrahydrofuran, (**d**) Allopurinol (control). The ligand refers to the stick model in magenta color. Redline is represented hydrophobic interaction between ligand and residues of the receptor.

tural and conformational changes of the ligand-receptor complex (Qashqoosh et al. 2019). Therefore, this method is employed to find the viewpoints of physical and chemical properties regarding the binding action of *M. oleifera* into the moiety of XO.

In order to perform molecular docking, protein target (receptor) and promising drugs (ligand) are required to be prepared. As for receptor molecules, the crystal structure of XO was retrieved from the protein database (PDB: 1v97) (Okamoto et al. 2004). Meanwhile, the extracted *M. oleifera* was employed as the ligand molecules. From our docking simulations, the binding energies and the binding pose between ligands and receptors were obtained and presented in Table 4 and Fig. 7, respectively. Further, the details of molecular interaction consisting of hydrogen bonds and hydrophobic interactions between the ligands-receptor complexes were provided in Table 5 and Fig. 8, respectively.

In this research, only the primary compounds of *M. oleifera*, i.e., 5-O-acetyl-thio-octyl-β-L-rhamnofuranoside, quinic acid, and 2-dimethyl(trimethylsilylmethyl)silyloxymethyltetrahydrofuran, were selected to become the ligand molecules. It was not easy to simulate three ligands simultaneously in docking protocols because ligands may overlap on each atom causing structural changes from the initial configuration. Molecular docking was performed separately for each ligand, and overall results were combined to create one configuration because of the similar receptor (XO) to overcome this issue.

Three ligands, i.e., 5-O-acetyl-thio-octyl-β-L-rhamnofuranoside (PubChem ID: 537841), quinic acid (PubChem ID: 6508), 2-dimethyl(trimethylsilylmethyl)silyloxymethyltetrahydrofuran (PubChem ID: 559105) against XO are extracted from the PubChem database. The possibility of ligand binding to the receptor site is achieved when the binding energy of the ligand-receptor complex is a negative value. From our finding, three complexes were found with various binding energies, as listed in Table 4.

All ligands showed negative values binding energy which are -9.3 kcal/mol, -8.2 kcal/mol, and -10.6 kcal/mol for 5-O-acetyl-thio-octyl-β-L-rhamnofuranoside, quinic acid, and 2-dimethyl(trimethyl silylmethyl)silyloxymethyltetrahydrofuran consecutively, indicating that the ligands could bind to the receptor, forming a ligand-receptor complex. In addition to that, the ligands of all complexes have higher binding energies than allopurinol (a positive

control), with the binding energy of -6.6 kcal/mol. This finding revealed that those 3 ligands found in the extract of *M. oleifera* leaves probably hold the potential as inhibitors for XO. Even though the inhibition activity of allopurinol is higher compared to the extract, the results still demonstrate that the *M. oleifera* leaves extracts containing those primary compounds could inhibit the XO enzyme. Thus, to identify the molecular interactions, including hydrogen bond and hydrophobic interaction between ligand and receptor, the snapshot structure of those ligands was analyzed using PLIP server (Salentin et al. 2015) and LigPlot v.4.5.3 program packages (Wallace et al. 1995).

Fig. 8 illustrates the binding site and geometrical pocket of the ligands in complex with the receptor. The result of complex 1 was visualized from multiple dockings of the several ligands, then combined into one configuration. The lines in red, yellow, and cyan colours correspond to the compounds of 5-O-acetyl-thio-octyl-β-L-rhamnofuranoside, quinic acid, and 2-dimethyl(trimethylsilylmethyl)silyloxymethyltetrahydrofuran, respectively. Meanwhile, complex 2 was denoted from the positive control into the site of XO. Of this figure, hydrogen bond and hydrophobic interactions contributed to the binding of ligand into the receptor. The detailed hydrogen bonds for those complexes are listed in Table 5. It was found that 5-O-acetyl-thio-octyl-β-L-rhamnofuranoside of complex 1 participated in hydrogen bonds with residues Arg912, Gln1040, Ser1080, Ser1082 of the receptor. In quinic acid, the hydrogen bonds were made in the residues of Arg912, Arg912, Ala1079, Ser1080, Ser1080, Glu1261. For 2-dimethyl(trimethylsilylmethyl) silyloxymethyltetrahydrofuran, the hydrogen bonds were formed with the residues of Thr1083, Gly1260. Meanwhile, allopurinol shown in complex 2 participated in hydrogen bonds with residues Gly797, Phe798, Met1038, and Gln1194. On the other hand, the hydrophobic interactions between ligand and receptor are presented in Fig. 8. 5-O-acetyl-thio-octyl-β-L-rhamnofuranoside of complex 1 formed the hydrophobic interaction with residues of the receptor, including Met1038, Arg912, Gly799, Glu1261, Phe911, Phe798, Ala1079, Ser1080, Gly1260, Ala1078, Thr1083, Lys1045, Val1259, Ser1082, Leu1042, Gly1039, Gln1040, Gln1194, Gln112, and Cys150. For quinic acid, the hydrophobic interaction was presented by the ligand's interaction with residues of the receptor such as Met1038, Cys150, Gln112, Arg912, Phe798, Gly799, Phe911, Ala1078, Ala1079, Glu1261, Ser1080, Val1259, Lys104, Thr1083, Ser1082, Gln1010, Gln1194, and Gly1039. 2-Dimethyl(trimethylsilylmethyl)silyloxymethyltetrahydrofuran participated in hydrophobic interaction with residues of Gly799, Arg912, Gly1260, Gln1040, Glu1261, Gln1194, Ser1080, Ala1079, Ala1078, Phe914, Phe1009, Arg880, Glu802, Phe798, Gln767, and Met1038. Meanwhile, for allopurinol, the hydrophobic interaction was observed between ligand and residues, including Gly1039, Phe798, Gly797, Gly796, Arg912, Gln1040, Gln112, Gln1194, Cys150, and Met1038. From these results, all primary ligands in the extracted *M. oleifera* leaves may become stable structures since the hydrogen bonds are coordinated between ligand and receptor. Also, the compounds of 5-O-acetyl-thio-octyl-β-L-rhamnofuranoside, quinic acid, and 2-dimethyl(trimethylsilylmethyl)silyloxymethyltetrahydrofuran bound to the similar residues of allopurinol, indicated that those compounds have similar activity as an inhibitor for XO. Furthermore, in the paper presented by Okamoto and co-workers (Okamoto et al. 2004), the catalytic site of XO provided and visualized in the UniProt database (https://www.ebi.ac.uk/pdbe/entry/pdb/1v97/bound/MTE), which includes residues Gly797, Met1038, Phe798, Arg912, Glu1261, Ala1079, Ala1078, Ser1080, Gln1040, Val1081, Ser1082, Gly1039, Gln1194, Cys150, and Gln112, is a crucial target for inhibiting the XO. Thus, the ligand that can bind to one of these residues is assumed to have a potential drug for treating goat disease. From our simulations, each ligand is bound to those residues by hydrogen bond and hydrophobic interaction, indicating those compounds can become inhibitor XO.

Conclusions

The results of enzyme characterization showed that the optimum activity of the enzyme isolated from bovine milk is at pH of 6.5, substrate concentration of 0.1 mM, and reaction temperature of 35 °C. For XO enzyme inhibition, the increase in extract concentration linearly augmented the percentage of inhibition. Methanol extract of 160 mg/mL showed the highest inhibition value of 21.35%. These results indicate that the methanol extract of *M. oleifera* leaves has the potential as an XO inhibitor. Furthermore, computational analysis was performed to gain insight into the molecular interaction between the primary compounds of *M. oleifera* leaves, including 5-O-acetyl-thio-octyl-β-L-rhamnofuranoside, quinic acid, and 2-dimethyl(trimethylsilylmethyl)silyloxymethyltetrahydrofuran with XO using the molecular docking method. Our finding demonstrated that these compounds were bound to the catalytic sites of XO by hydrogen bonds and hydrophobic interaction, suggesting these primary compounds of *M. oleifera* leaves have pharmacology activities for inhibiting the XO.

Acknowledgements

The authors express gratitude to Hasanuddin University for funding this research through the PDU (Penelitian Dasar Unhas) 2019 grant, (Contract No. 1585/UN4.22/PT.01.03/2019). Moreover, we thank Paulina Taba for her proofreading assistance on our manuscript; Siti Rosida R Djakad and Nurul Fajriah for their assistance in the preparation of the sample, and Nurlely Fattah for allowing us permission to use the laboratory facilities in the Study Program of Fisheries Product Technology, Pangkep State Polytechnic of Agriculture.

References

Arwansyah A, Arif AR, Ramli I, Kurniawan I, Sukarti S, Nur Alam M, Manguntungi B (2021a) Molecular modelling on SARS-CoV-2 papain-like protease: an integrated study with homology modelling, molecular docking, and molecular dynamics simulations. SAR and QSAR in Environmental Research 32(9): 1–20. https://doi.org/10.1080/1062936X.2021.1960601

Arwansyah A, Arif AR, Syahputra G, Sukarti S, Kurniawan I (2021b) Theoretical studies of Thiazolyl-Pyrazoline derivatives as promising drugs against malaria by QSAR modelling combined with molecular docking and molecular dynamics simulation. Molecular Simulation 47(12): 1–14. https://doi.org/10.1080/08927022.2021.1935926

Blaney JM, Dixon JS (1993) A good ligand is hard to find: Automated docking methods. Perspectives in Drug Discovery and Design 1(2): 301–319. https://doi.org/10.1007/BF02174531

Boopathi NM, Raveendran M (2021) Moringa and Its Importance. In: Boopathi NM, Raveendran M, Kole C (Eds) The Moringa Genome. Compendium of Plant Genomes. Springer, Cham, 1–9. https://doi.org/10.1007/978-3-030-80956-0_1

Bou-Salah L, Benarous K, Linani A, Bombarda I, Yousfi M (2020) In vitro and in silico inhibition studies of five essential oils on both enzymes human and bovine xanthine oxidase. Industrial Crops and Products 143: 111949. https://doi.org/10.1016/j.indcrop.2019.111949

Claaßen C, Gerlach T, Rother D (2019) Stimulus-Responsive Regulation of Enzyme Activity for One-Step and Multi-Step Syntheses. Advanced Synthesis and Catalysis 361(11): 2387–2401. https://doi.org/10.1002/adsc.201900169

DeLano WL (2002) Pymol: An open-source molecular graphics tool. CCP4 Newsletter on Protein Crystallography 40(1): 82–92. https://doi.org/10.4103/0974-8490.91028

Ezhilan BP, Neelamegam R (2012) GC-MS analysis of phytocomponents in the ethanol extract of Polygonum chinense L. Pharmacognosy Research 4(1): 11–14. https://doi.org/10.4103/0974-8490.91028

Fachriyah E, Ghifari MA, Anam K (2018) Isolation, Identification, and Xanthine Oxidase Inhibition Activity of Alkaloid Compound from *Peperomia pellucida*. IOP Conference Series: Materials Science and Engineering, 349(1): 012017. https://doi.org/10.1088/1757-899X/349/1/012017

Fejér J, Kron I, Pellizzeri V, Pľuchtová M, Eliašová A, Campone L, Gruľová D (2019) First report on evaluation of basic nutritional and antioxidant properties of *Moringa oleifera* Lam. from Caribbean Island of Saint Lucia. Plants 8(12): e537. https://doi.org/10.3390/plants8120537

Gliozzi M, Malara N, Muscoli S, Mollace V (2016) The treatment of hyperuricemia. International Journal of Cardiology 213: 23–27. https://doi.org/10.1016/j.ijcard.2015.08.087

Gong X, Shao J, Guo S, Pan J, Fan X (2020) Determination of inhibitory activity of Salvia miltiorrhiza extracts on xanthine oxidase with a paper-based analytical device. Journal of Pharmaceutical Analysis 11(5): 603–610. https://doi.org/10.1016/j.jpha.2020.09.004

Huang G, Chen S, Dai C, Sun L, Sun W, Tang Y, Ma H (2017) Effects of ultrasound on microbial growth and enzyme activity. Ultrasonics Sonochemistry 37: 144–149. https://doi.org/10.1016/j.ultsonch.2016.12.018

Huie CW (2002) A review of modern sample-preparation techniques for the extraction and analysis of medicinal plants. Analytical and bioanalytical chemistry 373(1): 23–30. https://doi.org/10.1007/s00216-002-1265-3

Jincy J, Sunil C (2020) Exploring antiulcer and anti-inflammatory activities of methanolic leaves extract of an Indian mistletoe *Helicantes elasticus* (Desv.) Danser. South African Journal of Botany 133: 10–16. https://doi.org/10.1016/j.sajb.2020.06.014

Kitchen DB, Decornez H, Furr JR, Bajorath J (2004) Docking and scoring in virtual screening for drug discovery: methods and applications. Nature Reviews Drug Discovery 3(11): 935–949. https://doi.org/10.1038/nrd1549

Kim KH, Kim YH, Lee KR (2007) Isolation of quinic acid derivatives and flavonoids from the aerial parts of *Lactuca indica* L. and their hepatoprotective activity in vitro. Bioorganic and medicinal chemistry letters 17(24): 6739–6743. https://doi.org/10.1016/j.bmcl.2007.10.046

Kostić DA, Dimitrijević DS, Stojanović GS, Palić IR, Dordević AS, Ickovski JD (2015) Xanthine oxidase: Isolation, assays of activity, and inhibition. Journal of Chemistry 2015: e294858. https://doi.org/10.1155/2015/294858

Ma ZF, Ahmad J, Zhang H, Khan I, Muhammad S (2020) Evaluation of phytochemical and medicinal properties of *Moringa* (*Moringa oleifera*) as a potential functional food. South African Journal of Botany 129: 40–46. https://doi.org/10.1016/j.sajb.2018.12.002

Maiuolo J, Oppedisano F, Gratteri S, Muscoli C, Mollace V (2016) Regulation of uric acid metabolism and excretion. International Journal of Cardiology 213: 8–14. https://doi.org/10.1016/j.ijcard.2015.08.109

Maobe MA, Nyarango RM, Box PO (2013) Fourier transformer infra-red spectrophotometer analysis of *Urtica dioica* medicinal herb used for the treatment of diabetes, malaria and pneumonia in Kisii region, Southwest Kenya. World Applied Sciences Journal 21(8): 1128–1135.

Marañón E, Lorenzo MP, Cermeño P, Mouriño-Carballido B (2018) Nutrient limitation suppresses the temperature dependence of phytoplankton metabolic rates. The ISME Journal 12(7): 1836–1845. https://doi.org/10.1038/s41396-018-0105-1

Meenakshi S, Umayaparvathi S, Arumugam M, Balasubramanian T (2011) In vitro antioxidant properties and FTIR analysis of two seaweeds of Gulf of Mannar. Asian Pacific Journal of Tropical Biomedicine 1(1): S66–S70. https://doi.org/10.1016/S2221-1691(11)60126-3

Mohos V, Pánovics A, Fliszár-Nyúl E, Schilli G, Hetényi C, Mladěnka P, Poór M (2019) Inhibitory effects of quercetin and its human and microbial metabolites on xanthine oxidase enzyme. International Journal of Molecular Sciences 20(11): e2681. https://doi.org/10.3390/ijms20112681

Monika, Sharma NK, Sheetal, Savitri Thakur N, Bhalla TC (2019) Xanthine oxidase of *Acinetobacter calcoaceticus* RL2-M4: Production, purification and characterization. Protein Expression and Purification 160: 36–44. https://doi.org/10.1016/j.pep.2019.03.014

Morris GM, Huey R, Lindstrom W, Sanner MF, Belew RK, Goodsell DS, Olson AJ (2009) AutoDock4 and AutoDockTools4: Automated docking with selective receptor flexibility. Journal of Computational Chemistry 30(16): 2785–2791. https://doi.org/10.1002/jcc.21256

Nam SY, Han NR, Rah SY, Seo Y, Kim HM, Jeong HJ (2018) Anti-inflammatory effects of *Artemisia scoparia* and its active constituent, 3, 5-dicaffeoyl-epi-quinic acid against activated mast cells. Immunopharmacology and Immunotoxicology 40(1): 52–58. https://doi.org/10.1080/08923973.2017.1405438

Natsir H, Chandra D, Rukayadi Y, Suhartono MT, Hwang JK, Pyun YR (2002) Biochemical characteristics of chitinase enzyme from *Bacillus* sp. of Kamojang Crater, Indonesia. Journal of Biochemistry, Molecular Biology, and Biophysics: JBMBB: The Official Journal of the Federation of Asian and Oceanian Biochemists and Molecular Biologists (FAOBMB) 6(4): 279–282.

Natsir H, Patong AR, Suhartono MT, Ahmad A (2010) Production and characterization of chitinase enzymes from sulili hot spring in south Sulawesi, *Bacillus* sp. HSA, 3-1a. Indonesian Journal of Chemistry 10(2): 256–260. https://doi.org/10.22146/ijc.21470

Natsir H, Wahab AW, Budi P, Arif AR, Arfah RA, Djakad SR, Fajriani N (2019) Phytochemical and Antioxidant Analysis of Methanol Extract of Moringa and Celery Leaves. Journal of Physics: Conference Series 1341(3): 032023. https://doi.org/10.1088/1742-6596/1341/3/032023

Natsir H, Wahab AW, Laga A, Arif AR (2018) Inhibitory activities of *Moringa oleifera* leaf extract against α-glucosidase enzyme in vitro. Journal of Physics: Conference Series 979(1): 012019. https://doi.org/10.1088/1742-6596/979/1/012019

O'Boyle NM, Banck M, James CA, Morley C, Vandermeersch T, Hutchison GR (2011) Open Babel: An open chemical toolbox. Journal of Cheminformatics 3(1): 1–14. https://doi.org/10.1186/1758-2946-3-33

Okamoto K, Matsumoto K, Hille R, Eger BT, Pai EF, Nishino T (2004) The crystal structure of xanthine oxidoreductase during catalysis: implications for reaction mechanism and enzyme inhibition. Proceedings of the National Academy of Sciences 101(21): 7931–7936. https://doi.org/10.1073/pnas.0400973101

Padayachee B, Baijnath H (2020) An updated comprehensive review of the medicinal, phytochemical and pharmacological properties of *Moringa oleifera*. South African Journal of Botany 129: 304–316. https://doi.org/10.1016/j.sajb.2019.08.021

Pero RW, Lund H, Leanderson T (2009) Antioxidant metabolism induced by quinic acid. Increased urinary excretion of tryptophan and nicotinamide. Phytotherapy Research: An International Journal Devoted to Pharmacological and Toxicological Evaluation of Natural Product Derivatives 23(3): 335–346. https://doi.org/10.1002/ptr.2628

Qashqoosh MTA, Manea YK, Alahdal FAM, Naqvi S (2019) Investigation of conformational changes of bovine serum albumin upon binding with benzocaine drug: A spectral and computational analysis. BioNanoScience 9(4): 848–858. https://doi.org/10.1007/s12668-019-00663-7

Rocchetti G, Blasi F, Montesano D, Ghisoni S, Marcotullio MC, Sabatini S, Lucini L (2019) Impact of conventional/non-conventional extraction methods on the untargeted phenolic profile of *Moringa oleifera* leaves. Food Research International 115: 319–327. https://doi.org/10.1016/j.foodres.2018.11.046

Rocchetti G, Pagnossa JP, Blasi F, Cossignani L, Piccoli RH, Zengin G, Lucini L (2020) Phenolic profiling and in vitro bioactivity of *Moringa oleifera* leaves as affected by different extraction solvents. Food Research International 127: 108712. https://doi.org/10.1016/j.foodres.2019.108712

Roche J, Royer CA (2018) Lessons from pressure denaturation of proteins. Journal of The Royal Society Interface 15(147): 20180244. https://doi.org/10.1098/rsif.2018.0244

Sagona WCJ, Chirwa PW, Sajidu SM (2020) The miracle mix of Moringa: Status of Moringa research and development in Malawi. South African Journal of Botany 129: 138–145. https://doi.org/10.1016/j.sajb.2019.03.021

Salentin S, Schreiber S, Haupt VJ, Adasme MF, Schroeder M (2015) PLIP: fully automated protein—ligand interaction profiler. Nucleic Acids Research 43(W1): W443–W447. https://doi.org/10.1093/nar/gkv315

Seth R, Asr K, Buchbinder R, Bombardier C, Cj E (2014) Allopurinol for chronic gout (Review). The Cochrane Library (10): 1–75. https://doi.org/10.1002/14651858.CD006077.pub3

Sharma NK, Thakur, S, Thakur, N, Savitri, Bhalla TC (2016) Thermostable Xanthine Oxidase Activity from *Bacillus pumilus* RL-2d Isolated from Manikaran Thermal Spring: Production and Characterization. Indian Journal of Microbiology 56(1): 88–98. https://doi.org/10.1007/s12088-015-0547-3

Singh AK, Rana HK, Tshabalala T, Kumar R, Gupta A, Ndhlala AR, Pandey AK (2020) Phytochemical, nutraceutical and pharmacological attributes of a functional crop *Moringa oleifera* Lam: An overview. South African Journal of Botany 129: 209–220. https://doi.org/10.1016/j.sajb.2019.06.017

Singh N, Kumar M, Miravet JF, Ulijn RV, Escuder B (2017) Peptide-Based Molecular Hydrogels as Supramolecular Protein Mimics. Chemistry - A European Journal 23(5): 981–993. https://doi.org/10.1002/chem.201602624

Sumaryada T, Arwansyah, Roslia AW, Ambarsari L, Kartono A (2016) Molecular docking simulation of mangostin derivatives and curcuminoid on maltase-glucoamylase target for searching anti-diabetes drug candidates. In 2016 1st International Conference on Biomedical Engineering (IBIOMED), 1–4. https://doi.org/10.1109/IBIOMED.2016.7869832

Tămaș M, Vostinaru O, Soran L, Lung I, Opris O, Toiu A, Mogosan C (2021) Antihyperuricemic, Anti-Inflammatory and Antihypertensive Effect of a Dry Extract from *Solidago virgaurea* L. (Asteraceae). Scientia Pharmaceutica 89(2): e27. https://doi.org/10.3390/scipharm89020027

Tian Y, Lin L, Zhao M, Peng A, Zhao K (2021) Xanthine oxidase inhibitory activity and antihyperuricemic effect of *Moringa oleifera* Lam. leaf hydrolysate rich in phenolics and peptides. Journal of Ethnopharmacology 270: 113808. https://doi.org/10.1016/j.jep.2021.113808

Trott O, Olson AJ (2010) AutoDock Vina: improving the speed and accuracy of docking with a new scoring function, efficient optimization, and multithreading. Journal of Computational Chemistry 31(2): 455–461. https://doi.org/10.1002/jcc.21334

Tshabalala T, Ndhlala AR, Ncube B, Abdelgadir HA, Van Staden J (2020) Potential substitution of the root with the leaf in the use of *Moringa oleifera* for antimicrobial, antidiabetic and antioxidant properties. South African Journal of Botany 129: 106–112. https://doi.org/10.1016/j.sajb.2019.01.029

Verma AK, Rajkumar V, Kumar MS, Jayant SK (2019) Antioxidative effect of drumstick (*Moringa oleifera* L.) flower on the quality and stability of goat meat nuggets. Nutrition and Food Science 50(1): 84–95. https://doi.org/10.1108/NFS-12-2018-0348

Wang GF, Shi LP, Ren YD, Liu QF, Liu HF, Zhang RJ, Zuo JP (2009) Anti-hepatitis B virus activity of chlorogenic acid, quinic acid and caffeic acid in vivo and in vitro. Antiviral research 83(2): 186–190. https://doi.org/10.1016/j.antiviral.2009.05.002

Wallace AC, Laskowski RA, Thornton JM (1995) LIGPLOT: a program to generate schematic diagrams of protein-ligand interactions. Protein Engineering, Design and Selection 8(2): 127–134. https://doi.org/10.1093/protein/8.2.127

White WB (2018) Gout, xanthine oxidase inhibition, and cardiovascular outcomes. Circulation 138(11): 1127–1129. https://doi.org/10.1161/CIRCULATIONAHA.118.036148

Zeng N, Zhang G, Hu X, Pan J, Zhou Z, Gong D (2018) Inhibition mechanism of baicalein and baicalin on xanthine oxidase and their synergistic effect with allopurinol. Journal of Functional Foods 50(July): 172–182. https://doi.org/10.1016/j.jff.2018.10.005

Zhang B, Li P, Zhang H, Wang H, Li X, Tian L, Zhang Q (2016) Preparation of lipase/Zn3(PO4)2 hybrid nanoflower and its catalytic performance as an immobilized enzyme. Chemical Engineering Journal 291: 287–297. https://doi.org/10.1016/j.cej.2016.01.104

Inhibitory effects of Moringa oleifera leaves extract on xanthine oxidase activity from bovine milk

ORIGINALITY REPORT

11%	9%	9%	%
SIMILARITY INDEX	INTERNET SOURCES	PUBLICATIONS	STUDENT PAPERS

PRIMARY SOURCES

1	repository.unhas.ac.id Internet Source	1%
2	assets.cureus.com Internet Source	1%
3	www.ijriar.com Internet Source	1%
4	Arwansyah Arwansyah, Abdur Rahman Arif, Irwan Ramli, Hasrianti Hasrianti et al. " Investigation of Active Compounds of In Treating Hypertension Using A Network Pharmacology - Based Analysis Combined with Homology Modeling, Molecular Docking and Molecular Dynamics Simulation ", ChemistrySelect, 2022 Publication	<1%
5	link.springer.com Internet Source	<1%
6	www.knowitall.com Internet Source	<1%

7	Selma Yildizhan. "Aphrodisiac Pheromones from the Wings of the Small Cabbage White and Large Cabbage White Butterflies, *Pieris rapae* and *Pieris brassicae*", ChemBioChem, 07/06/2009 Publication	<1 %
8	ijipls.com Internet Source	<1 %
9	pubag.nal.usda.gov Internet Source	<1 %
10	www.chemcas.net Internet Source	<1 %
11	www.tandfonline.com Internet Source	<1 %
12	Sidney J. Stohs, Michael J. Hartman. " Review of the Safety and Efficacy of ", Phytotherapy Research, 2015 Publication	<1 %
13	www.ijddr.in Internet Source	<1 %
14	kb.psu.ac.th Internet Source	<1 %
15	tel.archives-ouvertes.fr Internet Source	<1 %

16	Lin, Qisi, Ling Zhang, Dongzhi Yang, and Zhao Chunjie. "Contribution of Phenolics and Essential Oils to the Antioxidant and Antimicrobial Properties of Disporopsis pernyi (Hua) Diels", Journal of Medicinal Food, 2014. Publication	<1 %
17	Nur Zahirah Abd Rani, Khairana Husain, Endang Kumolosasi. "Moringa Genus: A Review of Phytochemistry and Pharmacology", Frontiers in Pharmacology, 2018 Publication	<1 %
18	assets.researchsquare.com Internet Source	<1 %
19	www.lookchem.cn Internet Source	<1 %
20	www.wjgnet.com Internet Source	<1 %
21	H Natsir, AW Wahab, P Budi, AR Arif, RA Arfah, SR Djakad, N Fajriani. "Phytochemical and Antioxidant Analysis of Methanol Extract of Moringa and Celery Leaves", Journal of Physics: Conference Series, 2019 Publication	<1 %
22	jouagr.qu.edu.iq Internet Source	<1 %

23	public.pensoft.net Internet Source	<1 %
24	M.S. Mokhele, D. Tswaledi, O. Aboyade, J. Shai, D. Katerere. "Investigation of Aloe ferox leaf powder on anti-diabesity activity", South African Journal of Botany, 2020 Publication	<1 %
25	environmentalchemistry.com Internet Source	<1 %
26	etd.adm.unipi.it Internet Source	<1 %
27	H Natsir, A W Wahab, A Laga, A R Arif. " Inhibitory activities of leaf extract against α-glucosidase enzyme in vitro ", Journal of Physics: Conference Series, 2018 Publication	<1 %
28	journal.unhas.ac.id Internet Source	<1 %
29	jpsr.pharmainfo.in Internet Source	<1 %
30	pdffox.com Internet Source	<1 %
31	sajs.co.za Internet Source	<1 %

32	Ângela Fernandes, Aducabe Bancessi, José Pinela, Maria Inês Dias et al. "Nutritional and phytochemical profiles and biological activities of Moringa oleifera Lam. edible parts from Guinea-Bissau (West Africa)", Food Chemistry, 2021 Publication	<1 %
33	Jintana Tragulpakseerojn, Ryuzaburo Yuki, Takuya Honda, Mariko Morii et al. "Apoptotic activities of the extract from *Moringa oleifera* leaves on human HCT116 colon cancer cells", Fundamental Toxicological Sciences, 2014 Publication	<1 %
34	K. Padmalochana. "Evaluation of the Antioxidant and Hepatoprotective Activity of Cryptolepis Buchanani", Journal of Applied Pharmaceutical Science, 2013 Publication	<1 %
35	mdpi-res.com Internet Source	<1 %
36	www.hindawi.com Internet Source	<1 %
37	www.kemikaliebranchen.dk Internet Source	<1 %
38	www.science.gov Internet Source	<1 %

39	"Natural Bio-active Compounds", Springer Science and Business Media LLC, 2019 Publication	<1 %
40	B. Padayachee, H. Baijnath. "An updated comprehensive review of the medicinal, phytochemical and pharmacological properties of Moringa oleifera", South African Journal of Botany, 2019 Publication	<1 %
41	Baoqiang Li, Ling Zhang, Kai Wang, Jie Yang. "Substrate-Based Design of Human Farnesyltransferase Peptide-like Pain Antagonists", International Journal of Peptide Research and Therapeutics, 2021 Publication	<1 %
42	Jiaoyan Ren, Linfeng Liao, Shuaiming Shang, Yamei Zheng, Wanqian Sha, Erdong Yuan. " Purification, Characterization, and Bioactivities of Polyphenols from (L.) Franco ", Journal of Food Science, 2019 Publication	<1 %
43	Mohsen Akbaribazm, Mohammad Rasoul Khazaei, Mozafar Khazaei. "Phytochemicals and antioxidant activity of alcoholic/hydroalcoholic extract of Trifolium pratense", Chinese Herbal Medicines, 2020 Publication	<1 %

44	Mónica A. Valdez-Solana, Verónica Y. Mejía-García, Alfredo Téllez-Valencia, Guadalupe García-Arenas et al. " Nutritional Content and Elemental and Phytochemical Analyses of Grown in Mexico ", Journal of Chemistry, 2015 Publication	<1 %
45	Sha Wang, Zhi-Yang Dong, Yong-Bin Yan. "Formation of High-Order Oligomers by a Hyperthemostable Fe-Superoxide Dismutase (tcSOD)", PLoS ONE, 2014 Publication	<1 %
46	T. Ahmadu, K. Ahmad, S. I. Ismail, O. Rashed, N. Asib, D. Omar. "Antifungal efficacy of Moringa oleifera leaf and seed extracts against Botrytis cinerea causing gray mold disease of tomato (Solanum lycopersicum L.)", Brazilian Journal of Biology, 2020 Publication	<1 %
47	Xiang Liu, Huitao Feng, Jie Wu, Kelin Xia. "Dowker complex based machine learning (DCML) models for protein-ligand binding affinity prediction", PLOS Computational Biology, 2022 Publication	<1 %
48	Yu Chen, Liyong Luo, Shanshan Hu, Renyou Gan, Liang Zeng. "The chemistry, processing, and preclinical anti-hyperuricemia potential of	<1 %

tea: a comprehensive review", Critical Reviews in Food Science and Nutrition, 2022
Publication

49	bmrb.cerm.unifi.it Internet Source	<1 %
50	downloads.hindawi.com Internet Source	<1 %
51	git.embl.de Internet Source	<1 %
52	greenpharmacy.info Internet Source	<1 %
53	www.florajournal.com Internet Source	<1 %
54	www.mdpi.com Internet Source	<1 %
55	www.worldnewsnaturalsciences.com Internet Source	<1 %
56	Tatiane Luiza Cadorin Oldoni, Nathalie Merlin, Mariéli Karling, Solange Teresinha Carpes et al. "Bioguided extraction of phenolic compounds and UHPLC-ESI-Q-TOF-MS/MS characterization of extracts of Moringa oleifera leaves collected in Brazil", Food Research International, 2019 Publication	<1 %

57	Rodgman, . "Sequence of CAS Registry Numbers for Components Identified in Tobacco, Tobacco Smoke, and Tobacco Substitute Smoke", The Chemical Components of Tobacco and Tobacco Smoke Second Edition, 2013. Publication	<1 %
58	Talat Bilal Yasoob, Abdur Rauf Khalid, Zhen Zhang, Xiaofeng Zhu, Suqin Hang. "Liver transcriptome of rabbits supplemented with oral Moringa oleifera leaf powder under heat stress is associated with modulation of lipid metabolism and up-regulation of genes for thermo-tolerance, antioxidation, and immunity", Nutrition Research, 2022 Publication	<1 %
59	www.deepdyve.com Internet Source	<1 %

Exclude quotes	On	Exclude matches	< 5 words
Exclude bibliography	On		